Bull. Chem. Soc. Jpn., 58, 2900—2910 (1985) [Vol. 58, No. 10

Reactions of NH Radicals. V. Photolysis of HN_3 in the Presence of C_3H_8 at 313 nm

Sukeya KODAMA*

Department of Applied Chemistry, College of Engineering, University of Osaka Prefecture, Sakai, Osaka 591

(Received September 5 , 1983)

The photolysis of HN_3 vapor in the presence of C_3H_8 was studied at 313 nm and 30 °C. The main products were N_2, H_2, CH_4, C_2H_6, C_3H_6, NH_4N_3, $CH_3NH_2\cdot HN_3$, $C_2H_5NH_2\cdot HN_3$, and *n*- and *i*-$C_3H_7NH_2\cdot HN_3$. The quantum yields of these products were measured as a function of the pressure of HN_3 or C_3H_8. The following mechanisms for the main reactions was proposed: $HN_3+h\nu(313\ \mathrm{nm})\rightarrow N_2+NH(a^1\Delta)$; $NH(a^1\Delta)+HN_3\rightarrow 2N_2+2H$, NH_2+N_3, and $N_2+N_2H_2^*$ (2); $NH(a^1\Delta)+C_3H_8\rightarrow C_3H_7NH_2^*$(*n*- and *i*-propylamine) (3); $NH(a^1\Delta)+C_3H_8\rightarrow NH(X^3\Sigma^-)+C_3H_8$ (4); $C_3H_7NH_2^*\rightarrow CH_3+C_2H_4NH_2$ (5); $CH_4+C_2H_4NH$ (6), $C_2H_4+CH_3NH_2$ (7), $C_2H_5+CH_2NH_2$ (8), $C_2H_6+CH_2NH$ (9), $H_2+C_3H_6NH$ (10), and $NH_3+C_3H_6$ (11); $C_3H_7NH_2^*+HN_3\rightarrow C_3H_7NH_2+HN_3$ (12); $C_3H_7NH_2^*+C_3H_8\rightarrow C_3H_7NH_2+C_3H_8$ (13). The rate constant ratios are: $k_3/k_2=1.28$; $k_4/k_2=0.262$; $k_6/k_5=0.109$; $k_7/k_5=0.050$; $k_8/k_5=1.39$; $k_9/k_5=0.040$; $k_{10}/k_5=1.20$; $k_{11}/k_5=4.72$; $k_{12}/k_5=666\ \mathrm{dm^3\ mol^{-1}}$; $k_{13}/k_5=860\ \mathrm{dm^3\ mol^{-1}}$. The formation ratio of *n*-$C_3H_7NH_2$/*i*-$C_3H_7NH_2$ was 1.55, regardless of the total pressure. The half-life of 1.78×10^{-10} s for $C_3H_7NH_2^*$ was obtained by using the collision theory. The relative and absolute rate constants were compared for the reactions of $NH(a^1\Delta)$ with CH_4, C_2H_6, and C_3H_8; it was found that the relative yield for the insertion of $NH(a^1\Delta)$ into a C–H bond increases with a decrease in the C–H bond dissociation energy.

The reactions of $NH(a^1\Delta)$ with HN_3,[1] Xe,[1] C_2H_6,[2] C_2H_4,[3] and CH_4[4] have been studied previously. It was found that HN_3 is a useful source for the first excited singlet $NH(a^1\Delta)$ and that $NH(a^1\Delta)$ reacts to give amine by insertion into a C–H bond, such as CH_3NH_2 from CH_4[4] and $C_2H_5NH_2$ from C_2H_6.[2] It is of interest to compare the relative reactivities for the reactions of $NH(a^1\Delta)$ with simple saturated hydrocarbons, such as CH_4, C_2H_6, C_3H_8, and *i*-C_4H_{10}, and to compare the relative efficiencies of the insertion per C–H bond for primary, secondary, and tertiary C–H bonds.

For the reactions of NH with saturated hydrocarbons, Miller[5] has studied the photolysis of HN_3 in the presence of CH_4, C_3H_8, *n*-C_4H_{10}, *i*-C_4H_{10}, and $(CH_3)_4C$, and measured the amines formed by the reactions of NH with these hydrocarbons. He has found that the amine yield increases in this order: $C_3H_8<$*n*-$C_4H_{10}<$*i*-$C_4H_{10}<(CH_3)_4C$. Back *et al.* have studied the flash photolysis of HNCO in the presence of C_3H_8[6] and the steady photolysis of HNCO with C_2H_6, C_3H_8, and $(CH_3)_4C$ at 51 °C.[7] They have found that the yield of CO was reduced to about one-third of its value in pure HNCO, the yield of N_2 was reduced close to zero, and the yield of H_2 was markedly enhanced in the presence of parafins. However, no amines could be detected. Thus, they suggested the decomposition of the vibrationally excited amines formed by insertion reactions. Richardson and Setser[8] have studied the thermal decomposition of HN_3 in the presence of CH_4, C_2H_6, and C_3H_8. However, no evidence was found for the reaction of NH with these hydrocarbons in the temperature range from 285 to 470 °C. Konar *et al.*[9] have investigated the photolysis of HN_3 in the presence of C_2H_6 and *i*-C_4H_{10} at 214 nm and room temperature, and showed that the formation rates of N_2 and H_2 decrease with an increase in the hydrocarbon pressure.

Recently, Tsunashima *et al.*[10] have studied the photolysis of HN_3 in liquid ethane, propane, and isobutane at the Dry Ice–methanol temperature, they have found the formation of ethylamine from C_2H_6, propyl- and isopropylamine from C_3H_8, and of butyl- and *t*-butylamine from *i*-C_4H_{10}. They have also estimated that the relative efficiencies of the insertion of ^{1}NH into primary, secondary, and tertiary C–H bonds are 1.0, 1.9, and 2.3 respectively. Hamada *et al.*[11] have studied the photolysis of HN_3 in liquid cyclopropane and in binary solutions of ethane and cyclopropane at the Dry Ice–methanol temperature, and reported that the insertion rate of $NH(a^1\Delta)$ into a C–H bond of cyclopropane is 1.05 times faster than that of ethane.

Kajimoto and Fueno[12] have studied the photolysis of HN_3 with C_2H_6 in the gas phase at 254 nm. From the pressure dependences of the yields of the insertion product($C_2H_5NH_2$) and the fragmentation products (CH_3 and C_2H_5), they have found that the branching ratios for three pathways of the insertion of $NH(a^1\Delta)$ into a C–H bond of C_2H_6, the hydrogen abstraction from C_2H_6 by $NH(a^1\Delta)$, and the electronic quenching of $NH(a^1\Delta)$ to $NH(X^3\Sigma^-)$ were 0.6, 0.1, and 0.3 respectively. Kondo *et al.*[13] have studied the effects of the reactions of $NH(a^1\Delta)$ with C_3H_8 on the photolysis of HN_3 at 254 nm, and determined that the relative secondary/primary C–H bond reactivity per bond is 1.5 for the insertion and 7.5 for the abstraction, results based on the pressure dependence of the yields of the insertion products (*n*-$C_3H_7NH_2$ and *i*-$C_3H_7NH_2$) and the fragmentation products (C_2H_5, *n*-C_3H_7, and *i*-C_3H_7).

In order to compare the specific rates for the insertion of $NH(a^1\Delta)$ into C–H bonds of simple saturated hydrocarbons, the collisional deactivations of $NH(a^1\Delta)$ to $NH(X^3\Sigma^-)$ by the hydrocarbons, and the unimolecular decomposition of the alkylamines formed by the insertion, the photolysis of HN_3 in the presence of C_3H_8 was investigated in this work, a continuation of our earlier studies with C_2H_6[2] and CH_4.[4]

Experimental

The propane obtained from the Takachiho Chemical Co. was 99.8% pure. It was purified each time before use by means of condensation and evacuation at the temperature of liquid nitrogen. The preparation and purification of HN_3, and the apparatus and procedure for the reaction, were the same as have been described previously.[1,2] All the runs in this work were carried out at 313 nm and 30 °C. The light intensity was reduced by screens to eliminate radical–radical reactions. The irradiation time was usually 90 min, and the degree of conversion of HN_3 was below 3 per cent.

The detected reaction products were N_2, H_2, CH_4, C_2H_4, C_2H_6, C_3H_6, CH_3N_3, NH_4N_3, $CH_3NH_2 \cdot HN_3$, $C_2H_5NH_2 \cdot HN_3$, and *n*- and *i*-$C_3H_7NH_2 \cdot HN_3$. No HCN was detected in the analysis by the pyridine-pyrazolone method.[14]

In order to inspect the radical intermediates, the products formed by the photolysis of HN_3 with C_3H_8 and NO at 313 nm were analysed gas chromatographically by the use of a Silicone SE-30 1-m column at room temperature. The retention times of these products (RNO_x) were then compared with those of the products formed on the photolyses of $CH_3N_2CH_3$, $C_2H_5COC_2H_5$, $(i\text{-}C_3H_7)_2CO$, and $n\text{-}C_3H_7COCH_3$ with NO, in the same gas chromatographic conditions. From the comparisons, the formations of CH_3 and C_2H_5 radicals as intermediates were confirmed, but few $n\text{-}C_3H_7$ or $i\text{-}C_3H_7$ radicals were found. The photolysis of HN_3 with C_3H_8 and NO at 254 nm was also carried out in order to inspect the effect of the wavelength. Thus, the large two peaks for $i\text{-}C_3H_7$ radicals, together with the peaks for the CH_3, C_2H_5, and $n\text{-}C_3H_7$ radicals, were found. The results at 254 nm are in accord with the results of Kondo *et al.*,[13] except that they did not detect any CH_3 radicals.

For the identification of the nitrogen-containing products, white volatile products condensed at the Dry Ice-acetone temperature were introduced into a solid sodium hydroxide column in order to remove the HN_3 from the white volatile products.[2,10] A mass spectrum of the HN_3-removed products at the ionizing voltage of 15 V is shown in Fig. 1. The mass spectra of the *n*- and $i\text{-}C_3H_7NH_2$ samples were also observed at the ionizing voltage of 15 V. In the spectra, the large peaks of $m/z=30$ ($CH_2NH_2^+$) for $n\text{-}C_3H_7NH_2$ and of $m/z=44$ ($CH_3CHNH_2^+$) for $i\text{-}C_3H_7NH_2$ were found, together with the parent-molecule-ion ($C_3H_7NH_2^+$) peak and its protonated-ion ($C_3H_7NH_3^+$) peak.

The product peaks of $m/z=17$, 18, 31, 32, 45, 46, 59, and 60 in Fig. 1 correspond to NH_3^+, NH_4^+, $CH_3NH_2^+$, $CH_3NH_3^+$, $C_2H_5NH_2^+$, $C_2H_5NH_3^+$, $C_3H_7NH_2^+$, and $C_3H_7NH_3^+$ respectively. The large peak of $m/z=30$ ($CH_2NH_2^+$) seems to arise from the electron-impact reactions of $CH_3NH_2 \rightarrow H + CH_2NH_2^+ + e^-$, as found in the mass spectrum of CH_3NH_2,[2,4,15] and of $n\text{-}C_3H_7NH_2 \rightarrow C_2H_5 + CH_2NH_2^+ + e^-$, as observed in the spectrum of the $n\text{-}C_3H_7NH_2$ sample. Similarly, the large peak of $m/z=44$ may be due to the electron-impact reactions of $C_2H_5NH_2 \rightarrow H + C_2H_4NH_2^+ + e^-$ and $i\text{-}C_3H_7NH_2 \rightarrow CH_3 + CH_3CHNH_2^+ + e^-$. The peak of $m/z=58$ may result from the $C_3H_7NH_2 \rightarrow H + C_3H_6NH_2^+ + e^-$ reaction.

For the quantitative analyses of the reaction products, first, these products were separated at the temperature of solid nitrogen (about −220 °C), −160 °C, and the Dry Ice-acetone temperature. Quantitative separations of N_2, H_2, and CH_4 passing through a trap at −220 °C were carried out by the procedures described previously.[2] C_2H_4, C_2H_6, and a part of the unconverted C_3H_8, condensed at −220 °C, were collected into a Toepler gauge, and the total volume was determined. The separations of C_2H_4, C_2H_6, and C_3H_8 were carried out by gas chromatography using a silica-gel column (2 m) at 60 °C.

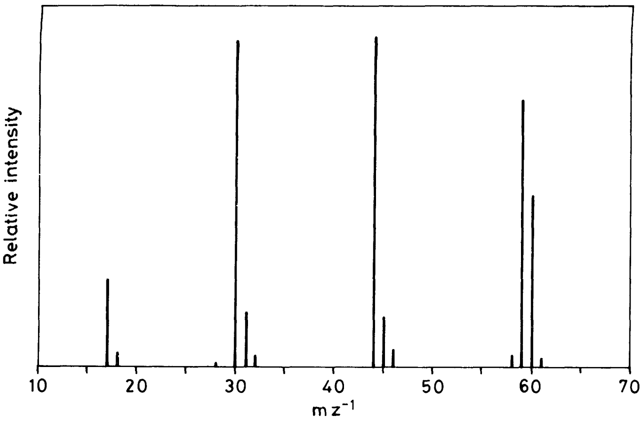

Fig. 1. Mass spectrum of the substances removed HN_3 from the white volatile products trapped at the Dry Ice–acetone temperature. The ionizing voltage is 15 V.

NH_4N_3 and the salts of amines with HN_3, condensed at the Dry Ice-acetone temperature, were introduced into a CuO column at about 550 °C. The amounts of N_2, NO, N_2O, and CO_2 produced as the combustion products were determined by a previously described method.[2] The total amount of nitrogen atoms, (N), is given by $(N)=2N_2+2N_2O+NO$. The total amount of carbon atoms in the products is identical with the amount of carbon dioxide formed by the combustion, (CO_2).

In order to determine the relative yields of CH_3NH_2, $C_2H_5NH_2$, $i\text{-}C_3H_7NH_2$, and $n\text{-}C_3H_7NH_2$, the HN_3-removed products were also analysed by means of gas chromatography at 10 °C using a 2-m columun of KOH (5%)-paraffin liquid (20%) coated on Chromosorb WAW.[16] The retention times of CH_3NH_2, $C_2H_5NH_2$, and $i\text{-}C_3H_7NH_2$ relative to $n\text{-}C_3H_7NH_2$ are 0,23, 0.36, and 0.56 respectively.

The quantum yields of the products were determined using HN_3 as an actinometer.[1]

Results

The photolysis of HN_3 of 6.7 kPa at 4.0 kPa of C_3H_8 was carried out as a function of the absorbed-light intensity in the range from 4.5 to 18.8×10^{14} quanta s^{-1}. The results, shown in Fig. 2, show that ϕ_{H_2} and ϕ_{CH_4} are independent of the light intensity, while ϕ_{N_2}, $\phi_{(N)}$, and $\phi_{(CO_2)}$ increase slightly with a decrease in the light intensity, but all the quantum yields converge to a constant value as the light intensity decreases.

The results for the photolysis of HN_3 of 6.7 kPa, measured as a function of the C_3H_8 pressure at the low absorbed-light intensity of 4.5×10^{14} quanta s^{-1}, are shown in Fig. 3. It may be seen in Fig. 3 that ϕ_{N_2} and ϕ_{H_2} decrease, $\phi_{(CO_2)}$ and $\phi_{(N)}$ increase, and ϕ_{CH_4}, $\phi_{C_2H_4}$, and

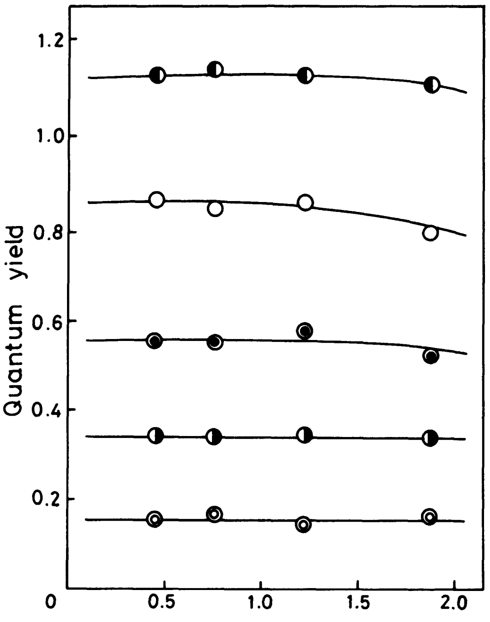

Fig. 2. Results for the photolysis of HN_3 of 6.7 kPa, measured as a function of the absorbed light intensity at 313 nm, 30 °C, and 4.0 kPa of C_3H_8. ◐, $\phi_{N_2}/3$; ○, $\phi_{(N)}/4$; ⊙, $\phi_{(CO_2)}$; ◑, ϕ_{H_2}; ◎, $4\phi_{CH_4}$.

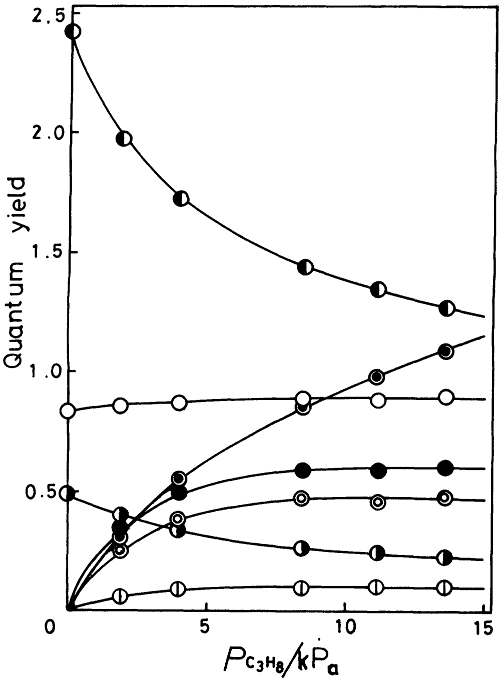

Fig. 3. Results of the photolysis of HN_3 of 6.7 kPa, measured as a function of C_3H_8 pressure at 313 nm, 30 °C, and the low absorbed light intensity of 4.5×10^{14} quanta s^{-1}. ◐, $\phi_{N_2}/2$; ⊙, $\phi_{(CO_2)}$; ○, $\phi_{(N)}/4$; ◑, ϕ_{H_2}; ◎, $10\phi_{CH_4}$; ●, $10\phi_{C_2H_6}$: ⦶, $50\phi_{C_2H_4}$.

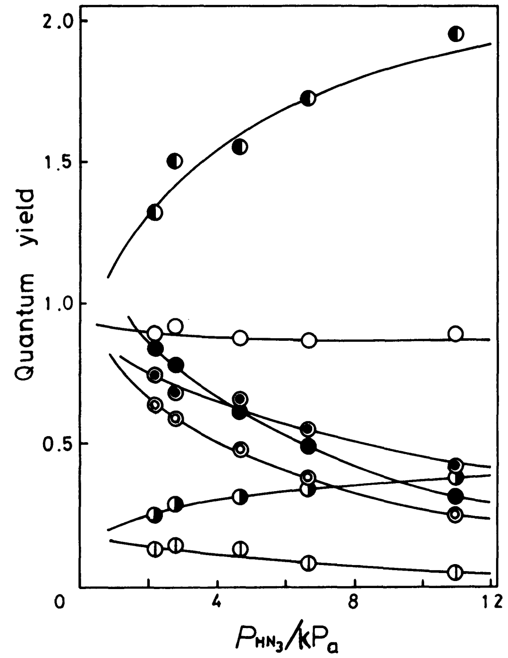

Fig. 4. Results of the photolysis measured as a function of HN_3 pressure at 4.0 kPa of C_3H_8, 30 °C, 313 nm, and the low incident light intensity of 3.9×10^{15} quanta s^{-1}. ◐, $\phi_{N_2}/2$; ⊙, $\phi_{(CO_2)}$; ○, $\phi_{(N)}/4$; ◑, ϕ_{H_2}; ◎, $10\phi_{CH_4}$; ●, $10\phi_{C_2H_6}$; ⦶, $50\phi_{C_2H_4}$.

$\phi_{C_2H_6}$ decrease *via* a maximum value at about 10 kPa as the C_3H_8 pressure increases.

Figure 4 shows the results of the photolysis measured as a function of the HN_3 pressure at 4.0 kPa of C_3H_8 and the low incident-light intensity of 3.9×10^{15} quanta s^{-1}. In Fig. 4, it is found that ϕ_{N_2} and ϕ_{H_2} increase, but $\phi_{(N)}$, $\phi_{(CO_2)}$, ϕ_{CH_4}, $\phi_{C_2H_4}$, and $\phi_{C_2H_6}$ decrease, with an increase in the HN_3 pressure.

On the photolysis of HN_3 of 6.7 kPa with C_3H_8 of 4.0 kPa and NO of 0.47 kPa at the absorbed-light intensity of 4.5×10^{14} quanta s^{-1}, the ϕ_{CH_4}, $\phi_{C_2H_6}$, and $\phi_{C_2H_4}$ values were 0.00374 (1/10.2 of that without NO), 0.00138 (1/35.6 of that without NO), and 0.00172 (the same as that without NO) respectively.

The amines obtained under the same experimental conditions as those in Figs. 3 and 4 were analysed by means of gas chromatography. Table 1 shows the yields of CH_3NH_2, $C_2H_5NH_2$, and n-$C_3H_7NH_2$ relative to that of i-$C_3H_7NH_2$. It may be seen in Table 1 that CH_3NH_2/i-$C_3H_7NH_2$ and $C_2H_5NH_2/i$-$C_3H_7NH_2$ decrease with an increase in the C_3H_8 or HN_3 pressure, while n-$C_3H_7NH_2/i$-$C_3H_7NH_2$ is constant regardless of the total pressure and the concentration ratio $[HN_3]/[C_3H_8]$.

Discussion

Reaction Mechanism. On the basis of the present experimental results and in the light of the results achieved by previous investigations,[1–4] the following reaction mechanism was postulated for the photolysis of HN_3 in the presence of C_3H_8, where A and P denote HN_3 and C_3H_8 molecules:

$$A + h\nu(313\,\text{nm}) \longrightarrow N_2 + NH(a^1\Delta) \qquad (1)$$

Table 1. Relative yields of amines

P_{HN_3} / kPa	$P_{C_3H_8}$ / kPa	CH_3NH_2 / i-$C_3H_7NH_2$	$C_2H_5NH_2$ / i-$C_3H_7NH_2$	n-$C_3H_7NH_2$ / i-$C_3H_7NH_2$
6.7	1.9	1.05	1.19	1.67
6.7	4.0	0.48	0.71	1.48
6.7	8.4	0.38	0.52	1.56
6.7	13.6		0.41	1.52
6.7	17.1	0.28	0.35	1.44
2.3	4.0		1.04	1.50
2.8	4.0	0.57	0.88	1.59
4.7	4.0		0.86	1.58
11.1	4.0	0.53	0.65	1.61

$$\mathrm{NH}(a^1\Delta) + \mathrm{A} \longrightarrow 2\mathrm{N_2} + 2\mathrm{H} \qquad (2a)$$

$$\mathrm{NH}(a^1\Delta) + \mathrm{A} \longrightarrow \mathrm{NH_2} + \mathrm{N_3} \qquad (2b)$$

$$\mathrm{NH}(a^1\Delta) + \mathrm{A} \longrightarrow \mathrm{N_2} + \mathrm{N_2H_2}^* \qquad (2c)$$

$$\mathrm{NH}(a^1\Delta) + \mathrm{P} \longrightarrow \mathrm{C_3H_7NH_2}^* \qquad (3)$$

$$\mathrm{NH}(a^1\Delta) + \mathrm{P} \longrightarrow \mathrm{NH}(X^3\Sigma^-) + \mathrm{P} \qquad (4)$$

$$\mathrm{C_3H_7NH_2}^* \longrightarrow \mathrm{CH_3} + \mathrm{C_2H_4NH_2} \qquad (5)$$

$$\mathrm{C_3H_7NH_2}^* \longrightarrow \mathrm{CH_4} + \mathrm{C_2H_4NH} \qquad (6)$$

$$\mathrm{C_3H_7NH_2}^* \longrightarrow \mathrm{C_2H_4} + \mathrm{CH_3NH_2} \qquad (7)$$

$$\mathrm{C_3H_7NH_2}^* \longrightarrow \mathrm{C_2H_5} + \mathrm{CH_2NH_2} \qquad (8)$$

$$\mathrm{C_3H_7NH_2}^* \longrightarrow \mathrm{C_2H_6} + \mathrm{CH_2NH} \qquad (9)$$

$$\mathrm{C_3H_7NH_2}^* \longrightarrow \mathrm{H_2} + \mathrm{C_3H_6NH} \qquad (10)$$

$$\mathrm{C_3H_7NH_2}^* \longrightarrow \mathrm{NH_3} + \mathrm{C_3H_6} \qquad (11)$$

$$\mathrm{C_3H_7NH_2}^* + \mathrm{A} \longrightarrow \mathrm{C_3H_7NH_2} + \mathrm{A} \qquad (12)$$

$$\mathrm{C_3H_7NH_2}^* + \mathrm{P} \longrightarrow \mathrm{C_3H_7NH_2} + \mathrm{P} \qquad (13)$$

$$\mathrm{CH_2NH_2} + \mathrm{A} \longrightarrow \mathrm{CH_3NH_2} + \mathrm{N_3} \qquad (14)$$

$$\mathrm{CH_2NH_2} + \mathrm{A} \longrightarrow \mathrm{CH_3N_3} + \mathrm{NH_2} \qquad (15)$$

$$\mathrm{H} + \mathrm{A} \longrightarrow \mathrm{H_2} + \mathrm{N_3} \qquad (16)$$

$$\mathrm{H} + \mathrm{A} \longrightarrow \mathrm{NH_2} + \mathrm{N_2} \qquad (17)$$

$$\mathrm{H} + \mathrm{P} \longrightarrow \mathrm{H_2} + \mathrm{C_3H_7} \qquad (18)$$

$$\mathrm{R_1}\ (\mathrm{R_1}=\mathrm{CH_3}, \mathrm{C_2H_5}, \mathrm{C_3H_7}, \mathrm{C_2H_4NH_2}) + \mathrm{A} \longrightarrow \mathrm{R_1H} + \mathrm{N_3} \qquad (19)$$

$$\mathrm{R_2NH_2}\ (\mathrm{R_2}=\mathrm{CH_3}, \mathrm{C_2H_5}, \mathrm{C_3H_7}) + \mathrm{A} \longrightarrow \mathrm{R_2NH_2}\cdot\mathrm{HN_3} \qquad (20)$$

$$\mathrm{R_3NH}\ (\mathrm{R_3}=\mathrm{CH_2}, \mathrm{C_2H_4}, \mathrm{C_3H_6}) + \mathrm{A} \longrightarrow \mathrm{R_3NH}\cdot\mathrm{HN_3}. \qquad (21)$$

The succeeding reactions for species consisting of only nitrogen and hydrogen atoms are as follows:[1] $\mathrm{NH}(X^3\Sigma^-)+\mathrm{A}\rightarrow\mathrm{H_2}+2\mathrm{N_2}$ (22); $\mathrm{NH}(X^3\Sigma^-)+\mathrm{A}\rightarrow\mathrm{NH_2}+\mathrm{N_3}$ (23); $\mathrm{N_2H_2}^*\rightarrow\mathrm{N_2H_2}^{**}$ (24); $\mathrm{N_2H_2}^*+\mathrm{A}\rightarrow\mathrm{N_2}+\mathrm{H_2}+\mathrm{A}$ (25); $\mathrm{N_2H_2}^*+\mathrm{A}\rightarrow\mathrm{NH_3}+2\mathrm{N_2}$ (26); $\mathrm{N_2H_2}^{**}+\mathrm{A}\rightarrow\mathrm{NH_3}+2\mathrm{N_2}$ (27); $\mathrm{NH_2}+\mathrm{A}\rightarrow\mathrm{NH_3}+\mathrm{N_3}$ (28); $\mathrm{NH_3}+\mathrm{A}\rightarrow\mathrm{NH_4N_3}$ (29); $\mathrm{N_3}+\mathrm{A}\rightarrow\mathrm{N_3}\cdot\mathrm{A}$ (30); $2\mathrm{N_3}\cdot\mathrm{A}\rightarrow3\mathrm{N_2}+2\mathrm{A}$ (31).

Since the formation of propyl- and isopropylamines has been confirmed by the gas-chromatographic and mass-spectrometric measurements, it is clear that the first excited singlet, NH($a^1\Delta$), formed by the photolysis of HN_3 at 313 nm[1] reacts to give propylamine upon insertion into a C–H bond of C_3H_8. The $C_3H_7NH_2^*$ formed by Reaction 3 implies vibrationally excited propylamine and isopropylamine, because both insertions into primary and secondary C–H bonds for C_3H_8 are possible.[10,11]

On the reactions of NH($a^1\Delta$) with C_3H_8 as a saturated hydrocarbon, a possible process other than the insertion is the collisional deactivation by C_3H_8 to NH($X^3\Sigma^-$). The collisional spin-relaxation process, Reaction 4, was also found for Xe,[1] CH_4,[4] and C_2H_6.[2] Kondo *et al.*[13] have proposed a hydrogen-abstraction reaction: $\mathrm{NH}(a^1\Delta)+\mathrm{C_3H_8}\rightarrow n\text{-}\mathrm{C_3H_7}$ or $i\text{-}\mathrm{C_3H_7}+\mathrm{NH_2}$, from C_3H_8 by NH($a^1\Delta$) upon photolysis at 254 nm. However, this reaction can be disregarded in the present work at 313 nm, because hardly no n-C_3H_7 or i-C_3H_7 radicals were formed. A non-abstraction mechanism is also supported by the fact that the intercept of the plot of NH_3/N_2 *vs.* $[HN_3]/[C_3H_8]$ is zero on the photolysis of HN_3 in liquid propane at from 250 to 320 nm.[10]

Reactions 5 and 8 show the unimolecular decompositions of $C_3H_7NH_2^*$ by the radical mechanism; they were established by the facts that CH_3 and C_2H_5 radicals were detected as intermediates and that ϕ_{CH_4} and $\phi_{C_2H_6}$ were reduced drastically in the presence of NO. The formations of CH_4, C_2H_4, and C_2H_6 from $C_3H_7NH_2^*$ by the molecular mechanism are represented by Reactions 6, 7, and 9; they are explainable by the facts that they are formed even in the presence of NO.

On the photolysis in the presence of NO, no drastical decrease for ϕ_{H_2} was observed. This suggests the formation of H_2 by a molecular mechanism such as

Reaction 10. Reaction 11 is supported by the fact that C_3H_6 was formed even in the presence of NO. Kondo *et al.*[13] have presented two fragmentation reactions, $n\text{-}C_3H_7NH_2^* \rightarrow n\text{-}C_3H_7 + NH_2$ and $i\text{-}C_3H_7NH_2^* \rightarrow i\text{-}C_3H_7 + NH_2$, in the photolysis at 254 nm. However, the fragmentations seem to be negligible in the photolysis at 313 nm, because scarcely no $n\text{-}C_3H_7$ or $i\text{-}C_3H_7$ radicals were detected. Reactions 12 and 13 are the collisional deactivation processes of $C_3H_7NH_2^*$ by HN_3 and C_3H_8 to give stable propyl- and isopropylamines, as was found for $C_2H_5NH_2^*$.[2]

Reaction 15 was introduced to explain the facts that the formation of CH_3N_3 was found and that the formation ratio $CH_3NH_2/C_2H_5NH_2$ is considerably less than $\phi_{C_2H_6}/\phi_{CH_4}$, although the yields of Reactions 6, 7, and 9 are very small as compared with those of Reactions 5 and 8. Reactions 14 and 15 were also found in the photolysis of HN_3 with C_2H_6.[2] Reaction 18 was introduced because the H atoms formed by Reaction 2a, exothermic with 370 kJ mol^{-1}, are in a "hot" state, and also because the rate of hydrogen abstraction from C_3H_8 by H atoms is much faster than that for C_2H_6.[17]

Reaction 19 is the hydrogen-abstraction reaction by CH_3, C_2H_5, C_3H_7, and $C_2H_4NH_2$ radicals from HN_3. Reaction 20 was supported by the experimental fact that basic amines (R_2NH_2) react with acidic HN_3 in the vapor phase to give the azide salts ($R_2NH_2 \cdot HN_3$) as a white volatile powder.[2]

Because of the unstable products, the chemical structures of the CH_2NH, C_2H_4NH, and C_3H_6NH formed by the molecular mechanisms of Reactions 6, 9, and 10 are not clear. However, these products (R_3NH) may have a basic imino or amino group, and they may be stabilized by forming the azide salts ($R_3NH \cdot HN_3$) with acidic HN_3, as in Reaction 21. The reactions other than those mentioned above have been discussed previously[1] and so are omitted here.

Reaction Kinetics. The reaction kinetics were carried out in order to confirm the mechanisms of Reactions 1 to 31, and in order to obtain the rate-constant ratios for these reactions. Since the formation ratio, $n\text{-}C_3H_7NH_2/i\text{-}C_3H_7NH_2$, is independent of the total pressure, as may be seen in Table 1, the ratio of collisional deactivation to unimolecular decomposition for $n\text{-}C_3H_7NH_2^*$ may be said to be the same as that for $i\text{-}C_3H_7NH_2^*$. Therefore, it is possible to treat the reaction kinetics for $n\text{-}C_3H_7NH_2^*$ and $i\text{-}C_3H_7NH_2^*$ collectively.

Regarding the formations of CH_4, C_2H_6, and C_2H_4, Eqs. I and II can be derived:

$$\phi_{C_2H_6}/\phi_{CH_4} = (k_8+k_9)/(k_5+k_6) \qquad \text{(I)}$$

$$\phi_{C_2H_4}/\phi_{CH_4} = k_7/(k_5+k_6) \qquad \text{(II)}$$

Plots of $\phi_{C_2H_6}/\phi_{CH_4}$ and $\phi_{C_2H_4}/\phi_{CH_4}$ *vs.* $[HN_3]/[C_3H_8]$ are shown in Fig. 5; both ratios are constant regardless of the $[HN_3]/[C_3H_8]$ ratio and the total pressure.

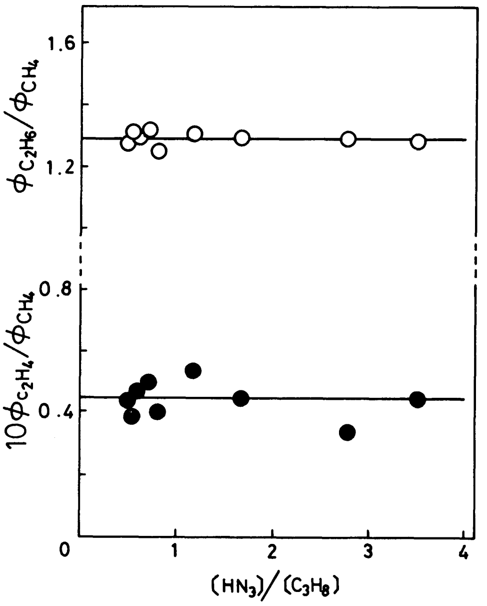

Fig. 5. Plots of $\phi_{C_2H_6}/\phi_{CH_4}$ (○) and $10\phi_{C_2H_4}/\phi_{CH_4}$ (●) *vs.* $[HN_3]/[C_3H_8]$.

When the quantum yields of CH_4 and C_2H_6 in the presence of NO, $\phi_{CH_4}(NO)$ and $\phi_{C_2H_6}(NO)$, are compared with those without NO, these relations:

$$\phi_{CH_4}(NO)/\phi_{CH_4} = k_6/(k_5+k_6) = 0.098 \qquad \text{(III)}$$

$$\phi_{C_2H_6}(NO)/\phi_{C_2H_6} = k_9/(k_8+k_9) = 0.028 \qquad \text{(IV)}$$

are obtained. From the values in Fig. 5 and Eqs. III and IV, $k_6/k_5=0.109$, $k_7/k_5=0.050$, $k_8/k_5=1.39$, and $k_9/k_5=0.040$ can be derived.

For the formations of CH_4 and (CO_2), Eq. V can be derived:

$$\frac{\phi_{(CO_2)}}{\phi_{CH_4}} = 2 + \frac{k_7+k_8k_{14}/(k_{14}+k_{15})+k_9+3k_{10}}{k_5+k_6} + \frac{3k_{12}[HN_3]}{k_5+k_6} + \frac{3k_{13}[C_3H_8]}{k_5+k_6} \qquad \text{(V)}$$

Plots of $\phi_{(CO_2)}/\phi_{CH_4}$ *vs.* P_{HN_3} or $P_{C_3H_8}$ are shown in Fig. 6. By using the $k_{15}/k_{14}=0.852$ obtained previously,[2] $k_{10}/k_5=1.20$, $k_{12}/k_5=666$ dm^3 mol^{-1}, and $k_{13}/k_5=860$ dm^3 mol^{-1} can be obtained from the intercepts and the slopes in Fig. 6.

Equation VI can be derived for the formations of N_2, H_2, (N), and CH_4:

$$\frac{\phi_{(N)}+3\phi_{H_2}-\phi_{N_2}}{3\phi_{CH_4}} = \frac{k_6+k_7+k_9+2k_{10}+k_{11}}{k_5+k_6} + \frac{k_{13}[M]}{k_5+k_6}, \qquad \text{(VI)}$$

where:

$$[M] = [C_3H_8] + (k_{12}/k_{13})[HN_3].$$

A plot of $(\phi_{(N)}+3\phi_{H_2}-\phi_{N_2})/3\phi_{CH_4}$ *vs.* P_M is shown in Fig. 7; $k_{11}/k_5=4.72$ was obtained from the intercept.

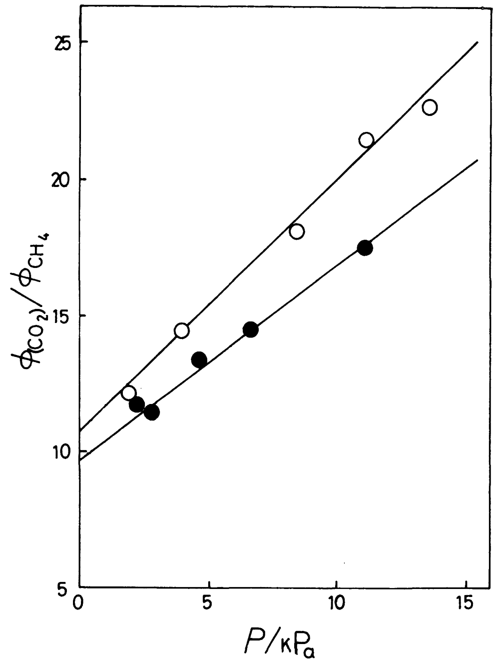

Fig. 6. Pressure dependences of $\phi_{(CO_2)}/\phi_{CH_4}$. ○, Measured as a function of C_3H_8 pressure at 6.7 kPa of HN_3; ●, measured as a function of HN_3 pressure at 4.0 kPa of C_3H_8.

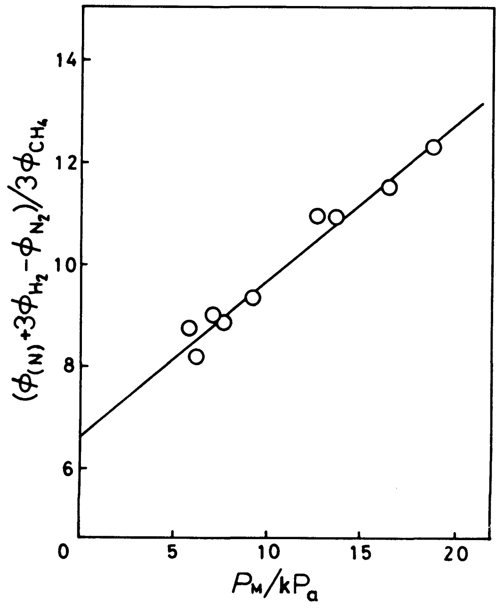

Fig. 7. Plot of $(\phi_{(N)}+3\phi_{H_2}-\phi_{N_2})/3\phi_{CH_4}$ *vs.* P_M.

Regarding the formation of amines, Eqs. VII and VIII can be derived:

$$\frac{CH_3NH_2}{C_2H_5NH_2}=\frac{k_7}{k_5}+\frac{k_8}{k_5}\frac{k_{14}}{k_{14}+k_{15}} \qquad \text{(VII)}$$

$$\frac{n\text{-}C_3H_7NH_2+i\text{-}C_3H_7NH_2}{C_2H_5NH_2}=\frac{k_{13}}{k_5}[M] \qquad \text{(VIII)}$$

Plots of $CH_3NH_2/C_2H_5NH_2$, $(n\text{-}C_3H_7NH_2+i\text{-}C_3H_7NH_2)/C_2H_5NH_2$, and $n\text{-}C_3H_7NH_2/i\text{-}C_3H_7NH_2$ *vs.* P_M are shown in Fig. 8. It may be found in Fig. 8 that the formation ratios of $CH_3NH_2/C_2H_5NH_2$ and $n\text{-}C_3H_7NH_2/i\text{-}C_3H_7NH_2$ are constant, regardless of the P_M, and that the $(n\text{-}C_3H_7NH_2+i\text{-}C_3H_7NH_2)/C_2H_5NH_2$ formation ratio is proportionate to P_M. The average value of the $n\text{-}C_3H_7NH_2/i\text{-}C_3H_7NH_2$ formation ratio was 1.55. The average value of $CH_3NH_2/C_2H_5NH_2$ is in accord with the value calculated using $k_7/k_5=0.050$, $k_8/k_5=1.39$, and $k_{15}/k_{14}=0.852$. The value of k_{13}/k_5 obtained from the slope in Fig. 8 is also consistent with those obtained from Figs. 6 and 7.

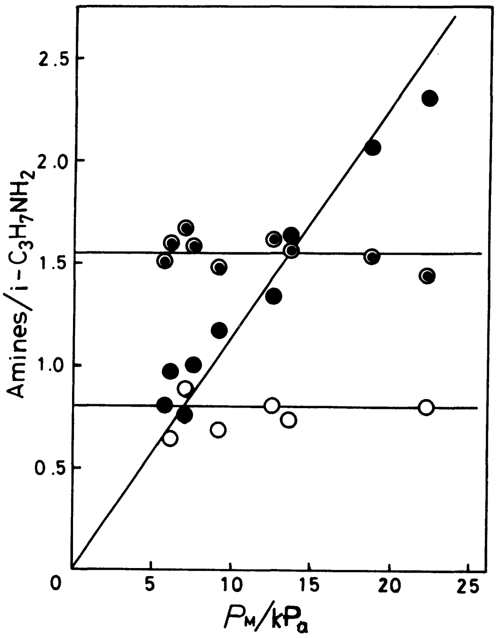

Fig. 8. Pressure dependences of $CH_3NH_2/C_2H_5NH_2$ (○), $n\text{-}C_3H_7NH_2/i\text{-}C_3H_7NH_2$ (◉), and $(n\text{-}C_3H_7NH_2+i\text{-}C_3H_7NH_2)/3C_2H_5NH_2$ (●).

Regarding the formation of N_2, H_2, (N), and CH_4, Eqs. IX and X can be derived:

$$\left(\frac{\phi_{H_2}+\phi_{(N)}/4}{\phi_{CH_4}}-\frac{k_{10}}{k_5+k_6}\right)\Big/\alpha =1+\frac{k_4}{k_3}+\frac{k_2+k_{2a}}{k_3}\frac{[HN_3]}{[C_3H_8]} \qquad \text{(IX)}$$

$$\left(\frac{\phi_{N_2}+\phi_{H_2}}{\phi_{CH_4}}-\frac{3k_5+3k_8+k_{10}}{k_5+k_6}\right)\Big/4\alpha =\frac{1}{4}+\frac{k_4}{k_3}+\frac{k_2+k_{2a}}{k_3}\frac{[HN_3]}{[C_3H_8]}, \qquad \text{(X)}$$

where:

$$k_2=k_{2a}+k_{2b}+k_{2c}$$

and:

$$\alpha=\frac{k_5+k_6+k_7+k_8+k_9+k_{10}+k_{11}+k_{12}[HN_3]+k_{13}[C_3H_8]}{k_5+k_6}.$$

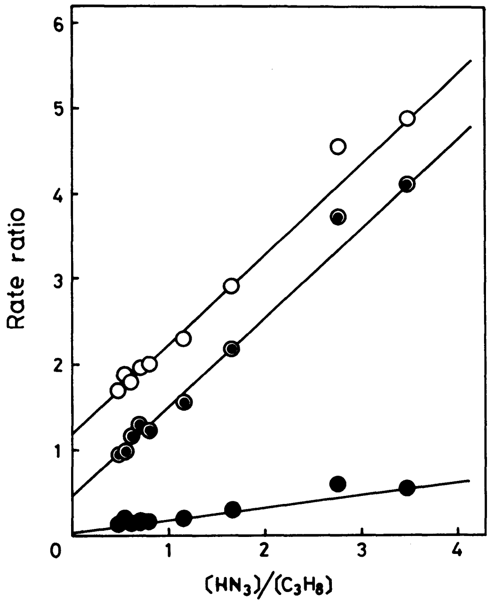

Fig. 9. Plots of the rate ratios *vs.* $[HN_3]/[C_3H_8]$. ○, $[(\phi_{H_2}+\phi_{(N)}/4)/\phi_{CH_4}-k_{10}/(k_5+k_6)]/\alpha$; ⊙, $[(\phi_{N_2}+\phi_{H_2})/\phi_{CH_4}-(3k_5+3k_8+k_{10})/(k_5+k_6)]/4\alpha$; ●, $[\phi_{H_2}/\phi_{CH_4}-k_{10}/(k_5+k_6)]/\alpha-\beta$.

Plots of $[(\phi_{H_2}+\phi_{(N)}/4)/\phi_{CH_4}-k_{10}/(k_5+k_6)]/\alpha$ and $[(\phi_{N_2}+\phi_{H_2})/\phi_{CH_4}-(3k_5+3k_8+k_{10})/(k_5+k_6)]/4\alpha$ *vs.* $[HN_3]/[C_3H_8]$ are shown in Fig. 9. From the intercept and the slope for Eq. IX and the $k_{2a}/k_2=0.336$ obtained previously,[1)] $k_3/k_2=1.28$ and $k_4/k_2=0.262$ were obtained. The same values were also obtained for Eq. X.

For the formations of H_2 and CH_4, Eq. XI can be derived:

$$\left(\frac{\phi_{H_2}}{\phi_{CH_4}}-\frac{k_{10}}{k_5+k_6}\right)\Big/\alpha-\beta=\frac{k_4}{k_3}\,\frac{k_{22}}{k_{22}+k_{23}}+\frac{k_{2c}}{k_3}\,\frac{k_{25}}{k_{24}/[HN_3]+k_{25}+k_{26}}\,\frac{[HN_3]}{[C_3H_8]},\qquad\text{(XI)}$$

where:

$$\beta=\frac{2k_{2a}}{k_3}\,\frac{k_{16}[HN_3]+k_{18}[C_3H_8]}{(k_{16}+k_{17})[HN_3]+k_{18}[C_3H_8]}\,\frac{[HN_3]}{[C_3H_8]}.$$

A plot of $[\phi_{H_2}/\phi_{CH_4}-k_{10}/(k_5+k_6)]/\alpha-\beta$ against $[HN_3]/[C_3H_8]$ is also shown in Fig. 9. The solid circles denote the values of $[\phi_{H_2}/\phi_{CH_4}-k_{10}/(k_5+k_6)]/\alpha-\beta$ calculated using the experimental values of ϕ_{H_2}/ϕ_{CH_4}. The lowest straight line represents the calculated values for the right side of Eq. XI. In these calculations, the values obtained above and the values obtained previously[1)] of $k_{2a}/k_2=0.336$, $k_{2c}/k_2=0.414$, $k_{17}/k_{16}=1.15$, $k_{23}/k_{22}=3.22$, $k_{24}/k_{25}=2.27\times10^{-4}$ mol dm^{-3}, and $k_{26}/k_{25}=1.19$ were used. As is shown in Fig. 9, the best fit for the experimental and calculated values was obtained when $k_{18}/k_{16}=0.51$.

Comparisons of Rate Constants. The specific rates of Reactions 12 and 13 can be estimated from these equations:

Table 2. Calculated values of k_z and k_5 at 30°C

M	σ_M	ε_{M-M}/k	k_z	$k_5(\eta=1)$
	Å	K	10^{14} cm^3 mol^{-1} s^{-1}	10^8 s^{-1}
HN_3	3.96$^{a)}$	240$^{a)}$	3.08	4.63
C_3H_8	4.84$^{b)}$	300$^{b)}$	3.90	4.53

a) Ref. 2. b) Ref. 19.

$$k_{12}=(\eta k_z)_{HN_3}\qquad\text{(XII)}$$

$$k_{13}=(\eta k_z)_{C_3H_8}.\qquad\text{(XIII)}$$

Here, k_z is the collision number of $C_3H_7NH_2^*$ per second and η is the collisional stabilization efficiency. The values of k_z can be calculated by means of the Lennard-Jones collision frequency:

$$k_z=N_A\sigma_{B-M}^2(8\pi kT/\mu_{B-M})^{1/2}\Omega_{B-M}^{(2.2)*},\qquad\text{(XIV)}$$

as has been described previously.[2)] The values of $\Omega_{B-M}^{(2.2)*}$ can conveniently be tabulated[18)] as a function of kT/ε_{B-M} with the Lennard-Jones well depth, $\varepsilon_{B-M}=(\varepsilon_{B-B}\varepsilon_{M-M})^{1/2}$. The σ_{B-M} is given by $\sigma_{B-M}=(\sigma_B+\sigma_M)/2$.

Assuming that the σ_B and ε_{B-B}/k values of n-$C_3H_7NH_2$ are the same as those of i-$C_3H_7NH_2$, the values of $\sigma_B=5.04$ Å and $\varepsilon_{B-B}/k=380$ K for both propyl- and isopropylamines were estimated in the light of those for n-C_4H_{10},[19)] i-C_4H_{10},[20)] n-C_3H_7OH,[21)] and $(CH_3)_2N$-NH_2.[22)] The calculated values of k_z at 30°C are shown in Table 2. The $(k_z)_{C_3H_8}/(k_z)_{HN_3}$ ratio is almost equal to the experimentally obtained ratio, $(k_{13}/k_5)/(k_{12}/k_5)$. This means that the $C_3H_7NH_2^*$ is deactivated with every collision ($\eta=1$), just as in the collisional deactivations by CO_2, HN_3, and C_2H_6 of $C_2H_5NH_2^*$.[2)] In the photolysis of HN_3 in liquid C_3H_8 at the Dry Ice-methanol temperature, no decomposition products of $C_3H_7NH_2^*$ formed by the insertion could be found.[10)] The main reason for this may be that the concentration of deactivator molecules is about 3500 times higher than that in the present system.

The absolute value of k_5 can be estimated from:

$$k_5=(\eta k_z)_{C_3H_8}/(k_{13}/k_5)_{obsd}.\qquad\text{(XV)}$$

It was estimated to be 4.53×10^8 s^{-1} from the calculated value of k_z for C_3H_8, the observed value of k_{13}/k_5, and $\eta=1$. Similarly, the absolute value of k_5 obtained from k_z for HN_3, the observed value of k_{12}/k_5, and $\eta=1$ was 4.63×10^8 s^{-1}, as is shown in Table 2. From the average value of $k_5=4.58\times10^8$ s^{-1} and the rate-constant ratios of k_6/k_5 and others, the absolute values of k_6, k_7, k_8, k_9, k_{10}, and k_{11} were estimated to be 0.50, 0.23, 6.4, 0.18, 5.5, and 21.6× 10^8 s^{-1} respectively. On the other hand, the rate-constant of the unimolecular decomposition of $C_2H_5NH_2^*$ formed by the reaction of $NH(a^1\Delta)$ with C_2H_6 was 9.8×10^9 s^{-1} for $C_2H_5NH_2^*\rightarrow CH_3+CH_2NH_2$ and 3.7×10^8 s^{-1} for $C_2H_5NH_2^*\rightarrow CH_3CN+2H_2$.[2)]

TABLE 3. RELATIVE REACTIVITIES FOR THE REACTIONS OF NH($a^1\Delta$) WITH X AT 30°C

X	k_r/k_2	k_d/k_2	$(k_r+k_d)/k_2$	k_d/k_r
HN_3[a]	1.000	0	1.000	0
Xe[a]	0	0.187	0.187	—
C_2H_4[b]	1.637	0	1.637	0
CH_4[c]	0.175	0.177	0.352	1.011
C_2H_6[d]	0.334	0.217	0.551	0.650
C_3H_8[e]	1.279	0.262	1.541	0.205

a) Ref. 1. b) Ref. 3. c) Ref. 4. d) Ref. 2. e) This work.

The half-life of $C_3H_7NH_2^*$ obtained from the $\tau=\ln 2/(k_5+k_6+k_7+k_8+k_9+k_{10}+k_{11})$ relation is 1.78×10^{-10} s. On the other hand, the half-life of $C_2H_5NH_2^*$ is 6.8×10^{-11} s.[2] Thus, the half-life of $C_3H_7NH_2^*$ is 2.6 times longer than that of $C_2H_5NH_2^*$. This trend is reasonable, because the rate of unimolecular decomposition decreases with an increase in the internal degree of freedom of the activated molecule.[23]

When the reactions of NH($a^1\Delta$) with a reactant (X) are represented by these general expressions:

$$\text{NH}(a^1\Delta) + \text{X} \longrightarrow \text{Products} \qquad k_r$$

$$\text{NH}(a^1\Delta) + \text{X} \longrightarrow \text{NH}(X^3\Sigma^-) + \text{X}, \quad k_d$$

the values of k_r/k_2, k_d/k_2, $(k_r+k_d)/k_2$, and k_d/k_r for C_3H_8 are shown in Table 3 together with those obtained previously.[1–4] It may be seen in Table 3 that k_r/k_2, k_d/k_2, and $(k_r+k_d)/k_2$ increase, but k_d/k_r decreases, with an increase in the carbon number in a saturated hydrocarbon molecule. Meanwhile, the k_r/k_2 ratio of the saturated hydrocarbons consisting of only the σ bond is, in general, low as compared with that of C_2H_4 having the π bond.

The values of $(k_r+k_d)/k_2$, $((k_r+k_d)/k_2)_{rel}$, $k_r/(k_r+k_d)$, and $(k_r/k_2)_{rel}$ for saturated hydrocarbons are shown in Table 4, where $((k_r+k_d)/k_2)_{rel}$ and $(k_r/k_2)_{rel}$ indicate the values of $(k_r+k_d)/k_2$ and k_r/k_2 relative to those of C_2H_6. It may be seen in Table 4 that the values of $((k_r+k_d)/k_2)_{rel}$, $k_r/(k_r+k_d)$, and $(k_r/k_2)_{rel}$ for our works are similar to those obtained by Tsunashima *et al.*[10] and by Kajimoto *et al.*[12,13] However, the values of $(k_r+k_d)/k_2$ obtained in the liquid phase by Tsunashima *et al.*[10] are much less than those in our works. The main reason for the large discrepancy seems to be due to the difference in phase (vapor and liquid), as has been discussed previously.[2] The values of $(k_r+k_d)/k_2$ obtained at 254 nm by Kajimoto *et al.*[12,13] are also small as compared with our values. This dissimilarity may be due to the effect of the wavelength.

The formation ratio of n-$C_3H_7NH_2$/i-$C_3H_7NH_2$ was 1.55, regardless of the total pressure. This ratio means that the insertion rate of NH($a^1\Delta$) into a secondary C–H bond of C_3H_8 is 1.94 times faster than that into a primary C–H bond. This value is well consistent with the value of 1.9 obtained by Tsunashima *et al.*[10] Kondo *et al.*[13] have obtained the insertion efficiency ratio of 1.5 in the photolysis at 254 nm. Tsunashima *et al.*[10] have also found that the insertion efficiency into a tertiary C–H bond of isobutane is 2.3 times higher than that for a primary C–H bond. In general, the insertion efficiency per C–H bond, ζ_i(C–H), can be represented by this equation:

$$\zeta_i(\text{C–H}) = f_i(k_r/k_2)_{\text{obsd}}/F, \qquad \text{(XVI)}$$

where $F=n_pf_p+n_sf_s+n_tf_t$. Here, n_p, n_s, and n_t indicate the number of primary, secondary, and tertiary C–H bonds respectively in a saturated hydrocarbon molecule. Similarly f_p, f_s, and f_t denote the relative efficiencies for the insertions into primary, secondary, and tertiary C–H bonds respectively. f_i means f_p, f_s, or f_t. If f_p is fixed as a basis, then f_p becomes unity.

The values of f_i, F, $(k_r/k_2)_{\text{obsd}}$, and ζ_i(C–H) are shown in Table 5, together with the ratio of the ζ_i(C–H) of X to the ζ_i(C–H) of CH_4, $\zeta_i(\text{C–H})_X/\zeta_p(\text{C–H})_{CH_4}$. The bond-dissociation energies of these C–H bonds, D_i(C–H), are also listed in Table 5. These bond-dissociation energies were calculated assuming that the standard heats of the formation of CH_4, C_2H_6, C_3H_8, i-C_4H_{10}, c-C_3H_6, H, CH_3, C_2H_5, n-C_3H_7, i-C_3H_7, i-C_4H_9, t-C_4H_9, and c-C_3H_5 were −74.9, −84.7, −103.8, −134.5, 53.3, 218.0, 145.2,[24] 117.2,[25] 87.9,[26] 73.6,[27] 58.6,[27] 35.1,[28] and 255.2[27] kJ mol^{-1} respectively. The plot of $\zeta_i(\text{C–H})_X/\zeta_p(\text{C–H})_{CH_4}$ *vs.* D_i(C–H) is shown in Fig. 10; it shows that $\zeta_i(\text{C–H})_X/\zeta_p(\text{C–H})_{CH_4}$ increases with a decrease in D_i(C–H), especially in the range lower than 420 kJ mol^{-1}. From the results shown in Fig. 10, it may be possible to predict the over-all insertion efficiency for reactions of NH($a^1\Delta$) with saturated hy-

TABLE 4. COMPARISONS OF $(k_r+k_d)/k_2$, $k_r/(k_r+k_d)$, AND k_r/k_2

X	$\dfrac{k_r+k_d}{k_2}$	$\left(\dfrac{k_r+k_d}{k_2}\right)_{rel}$	$\dfrac{k_r}{k_r+k_d}$	$\left(\dfrac{k_r}{k_2}\right)_{rel}$
CH_4	0.352[a]	0.64[a]	0.497[a]	0.524[a]
C_2H_6	0.551[a] 0.0093[b] 0.13[c]	1.00 1.00 1.00	0.606[a] 0.86[b] 0.7[c]	1.00 1.00 1.00
C_3H_8	1.54[a] 0.026[b] 0.45[c]	2.80[a] 2.78[b] 3.46[c]	0.830[a] 0.79[b] 0.95[c]	3.83[a] 2.6[b] 4.7[c]
i-C_4H_{10}	0.033[b]	3.58[b]	0.75[b]	3.1[b]
c-C_3H_6				1.05[d]

a) Refs. 2 and 4, and this work. b) Ref. 10. $(k_r+k_d)/k_2$ was calculated from their values of $k_r/(k_r+k_d)$ and k_2/k_r. c) Refs. 12 and 13. Included in k_r the specific rate of the abstraction reaction, NH($a^1\Delta$)+C_2H_6→NH_2+C_2H_5 or NH($a^1\Delta$)+C_3H_8→NH_2+C_3H_7. d) Ref. 11.

TABLE 5. INSERTION EFFICIENCIES PER C–H BOND

X	Type of C–H bond[a)]	f_i	F	$\left(\frac{k_r}{k_2}\right)_{obsd}$	ζ_i(C–H)	$\zeta_i(\text{C–H})_X / \zeta_p(\text{C–H})_{CH_4}$	D_i(C–H)[b)] / kJ mol^{-1}
CH_4	p	1	4	0.175[f)]	0.0438	1.000	438.0
C_2H_6	p	1	6	0.334[g)]	0.0557	1.272	419.8
C_3H_8	p	1	9.87	1.279[c)]	0.1296	2.959	409.7
	s	1.94[c)]			0.2508	5.727	395.5
c-C_3H_6	s	1[d)]	6	0.351[h)]	0.0585	1.337	419.9
i-C_4H_{10}	p	1	11.3	1.525[i)]	0.1350	3.082	411.1
	t	2.3[e)]			0.3104	7.088	387.6

a) p, s, and t denote the primary, secondary, and tertiary C–H bonds respectively. b) Calculated from the standard heats of the formation of hydrocarbons, H, and radicals; see text. c) This work. d) f_i was regarded as unity, because cycropropane has the secondary hydrogen alone. e) Ref. 10. f) Ref. 4. g) Ref. 2. h) Calculated from $(k_r(C_2H_6)/k_2)_{obsd}=0.334$ (Ref. 2) and $(k_r(c\text{-}C_3H_6)/k_r(C_2H_6))_{obsd}=1.05$ (Ref. 11). i) The value of 1.525 (0.334×3.83×3.1/2.6) was estimated from the data of $(k_r(C_2H_6)/k_2)_{obsd}=0.334$ (Ref. 2), $(k_r(C_3H_8)/k_2)_{rel}=3.83$ (Table 4), $(k_r(i\text{-}C_4H_{10})/k_2)_{rel}=3.1$ (Ref. 10), and $(k_r(C_3H_8)/k_2)_{rel}=2.6$ (Ref. 10).

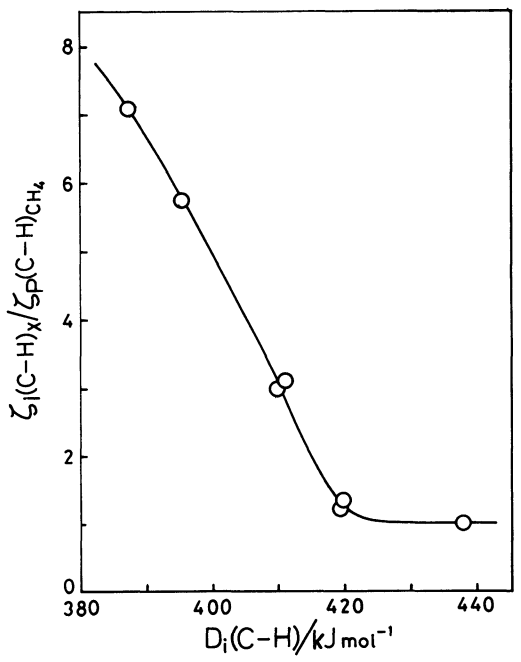

Fig. 10. Plot of $\zeta_i(\text{C-H})_X/\zeta_p(\text{C-H})_{CH_4}$ vs. D_i(C-H).

drocarbons.

The absolute value of k_2 which was observed by Piper, Krech, and Taylor,[29] k_2(PKT), is 1.084×10^{14} cm^3 mol^{-1} s^{-1}. If this value is applied, the absolute rate-constant for the over-all quenching of NH($a^1\Delta$) by X, k_q(X), can be calculated by this equation:

$$k_q(X) = \frac{(k_r+k_d)_X}{k_2} k_2(\text{PKT}). \qquad \text{(XVII)}$$

The values of k_q(X) calculated from $(k_r+k_d)_X/k_2$ in Table 3 and k_2(PKT) are shown in Table 6 ; the Table shows that k_q(X) increases with an increase in the carbon number in a X molecule.

On the other hand, the maximum rate-constant of the bimolecular reaction in the gas phase, k_b, can be calculated by this equation:[30]

$$k_b = \frac{2\Gamma(1-2/s)N_A}{\sigma}\left(\frac{2\pi kT}{\mu}\right)^{1/2}\left[\frac{(s-2)A}{2kT}\right]^{2/s}, \qquad \text{(XVIII)}$$

when the intermolecular attractive potential, u, is expressed by $u=-A/r^s$. The attractive potential constant, A, can be calculated from the dispersion term reported by Slater and Kirkwood[31] and the induction term for NH and X:

$$A = \frac{3he\alpha_{NH}\alpha_X}{4\pi m_e^{1/2}[(\alpha/N_e)_{NH}^{1/2}+(\alpha/N_e)_X^{1/2}]} + \alpha_X\mu_D(\text{NH})^2, \qquad \text{(XIX)}$$

as has been described previously.[3] The values of k_b calculated using $s=6$, $\Gamma(2/3)=1.354$, $\sigma=1$, $T=303$ K, $\alpha_{NH}=1.38\times10^{-24}$ cm^3,[32] $\mu_D(\text{NH})=1.627$ debye,[33] and $N_e(\text{NH})=6$ are shown in Table 6, together with $k_q(X)/k_b$. It may be found in Table 6 that k_b increases slightly with an increase in the carbon number in X, while $k_q(X)/k_b$ increases considerably from 1/10 for CH_4 to 1/2.6 for C_3H_8.

The absolute and relative quenching rates of $C(2^1D_2)$,[34,35] $O(2^1D_2)$,[36–38] $S(3^1D_2)$,[39,40] and CH_2 $(^1A_1)$[41,42] by CH_4, C_2H_6, C_3H_8, and others have been observed widely. These over-all quenching-rate constants are shown in Table 7, together with those for

TABLE 6. COMPARISONS OF k_q(X), k_b, AND $k_q(X)/k_b$ AT 303 K

X	k_q(X) / 10^{14} cm^3 mol^{-1} s^{-1}	α / 10^{-24} cm^3	N_e	A / 10^{-67} J cm^6	k_b / 10^{14} cm^3 mol^{-1} s^{-1}	$k_q(X)/k_b$
CH_4	0.382	2.60[a)]	8	92.9	3.83	0.0997
C_2H_6	0.597	4.48[b)]	14	160.7	4.05	0.148
C_3H_8	1.671	6.35[b)]	20	228.2	4.30	0.389

a) Ref. 18b, p. 950. b) P. Sliwinski, *Z. Phys. Chem. (Frankfurt am Main)*, **63**, 263 (1969).

Table 7. Comparisons of the over-all quenching-rate constants at about 300 K

Quencher	Quenching-rate constant/10^{-11} cm^3 molecule^{-1} s^{-1}				
	C(2^1D_2)	O(2^1D_2)	S(3^1D_2)	NH($a^1\Delta$)	CH_2($^1A_2$)
HN_3				18[a)]	
Xe	11[a)]	7.2[a)]	4.0[a)]	3.4[a)]	1.6[h)]
C_2H_4	37[a)]	35.6[a)]	25[a)]	29.5[a)]	15.0[i)]
CH_4	21.0[b)]	14.0[c)]	8.6[e)]	6.3[f)]	7.0[i)]
C_2H_6		26.0[a)]	4.3[a)]	9.9[a)]	19.0[i)]
C_3H_8		33.3[d)]		27.8[g)]	24.0[i)]

a) Ref. 3. b) Ref. 35. c) Ref. 38. d) Estimated from $k_q^{O(^1D)}(C_2H_6)=26.0\times10^{-11}$ cm^3 molecule^{-1} s^{-1} and $k_q^{O(^1D)}(C_3H_8)/k_q^{O(^1D)}(C_2H_6)=1.28$ (Ref. 37). e) Ref. 39. f) Ref. 4. g) This work. h) Ref. 41. i) Ref. 42.

NH($a^1\Delta$). Table 7 shows that the absolute quenching rates of NH($a^1\Delta$) by Xe, C_2H_4, CH_4, C_2H_6, and C_3H_8 are very similar to those of C($^1D_2$), O($^1D_2$), S($^1D_2$), and CH_2($^1A_1$), which are isoelectronic with NH($a^1\Delta$).

Summary. From the formation ratio of the n-$C_3H_7NH_2$ and i-$C_3H_7NH_2$ produced in the photolysis of HN_3 at 313 nm and 30 °C in the presence of C_3H_8, the insertion efficiency of NH($a^1\Delta$) into a secondary C–H bond of C_3H_8 was found to be 1.94 times higher than that of a primary C–H bond. The relative insertion efficiencies per C–H bond were 1.00 for CH_4, 1.27 for C_2H_6, 2.96(p) and 5.73(s) for C_3H_8, 1.34 for c-C_3H_6, and 3.08(p) and 7.09(t) for i-C_4H_{10}, judging from comparisons of the present and previous results.[2,4,10,11] Here, p, s, and t indicate the primary, secondary, and tertiary C–H bonds. The insertion efficiency per C–H bond increases with a decrease in the C–H bond dissociation energy. The insertion-rate constants, as estimated from the absolute reaction rate of NH($a^1\Delta$) with HN_3,[29] were 1.90, 3.62, and 13.9×10^{13} cm^3 mol^{-1}s^{-1} for CH_4, C_2H_6, and C_3H_8 respectively. The over-all quenching-rate constants of NH($a^1\Delta$) by CH_4, C_2H_6, C_3H_8, C_2H_4,[3] and Xe[1] were, respectively, 3.82, 5.97, 16.7, 17.7, and 2.03×10^{13} cm^{3}mol^{-1}s^{-1}; they were found to be very similar to those of C($^1D_2$), O($^1D_2$), S($^1D_2$), and CH_2($^1A_1$), which are isoelectronic with NH($a^1\Delta$).

The author is grateful to Mr. Jun Fukuchi for his cooperation.

References

1) S. Kodama, *Bull. Chem. Soc. Jpn.*, **56**, 2348 (1983).

2) S. Kodama, *Bull. Chem. Soc. Jpn.*, **56**, 2355 (1983).

3) S. Kodama, *Bull. Chem. Soc. Jpn.*, **56**, 2363 (1983).

4) S. Kodama, *Bull. Chem. Soc. Jpn.*, **58**, 2891 (1985).

5) E. D. Miller, Ph. D. Dissertation, Catholic University of America, Washington, D. C., 1961.

6) R. A. Back, *J. Chem. Phys.*, **40**, 3493 (1964).

7) J. L. Brash and R. A. Back, *Can. J. Chem.*, **43**, 1778 (1965).

8) W. C. Richardson and D. W. Setser, *Can. J. Chem.*, **47**, 2725 (1969).

9) R. S. Konar, S. Matsumoto, and B. deB. Darwent, *Trans. Faraday Soc.*, **67**, 1698 (1971).

10) S. Tsunashima, J. Hamada, M. Hotta, and S. Sato, *Bull, Chem. Soc. Jpn.*, **53**, 2443 (1980).

11) J. Hamada, S. Tsunashima, and S. Sato, *Bull. Chem. Soc. Jpn.*, **55**, 1739 (1982).

12) O. Kajimoto and T. Fueno, *Chem. Phys. Lett.*, **80**, 484 (1981).

13) O. Kondo, J. Miyata, O. Kajimoto, and T. Fueno, *Chem. Phys. Lett.*, **88**, 424 (1982).

14) J. M. Kruse and M. G. Mellon, *Anal. Chem.*, **25**, 446 (1953).

15) K. Fukui, I. Fujita, and K. Kuwata, *Bull. Chem. Soc. Jpn.*, **45**, 2278 (1972).

16) A. T. James, *Biochem. J.*, **52**, 242 (1952); A. T. James and A. J. P. Martin, *Analyst*, **77**, 915 (1952).

17) W. E. Jones, S. D. MacKnight, and L. Teng, *Chem. Rev.*, **73**, 407 (1973). The hydrogen-abstraction rate by H atoms from C_3H_8 is about ten times faster than that from C_2H_6 at 30 °C.

18) a) J. O. Hirschfelder, R. B. Bird, and E. L. Spotz, *J. Chem. Phys.*, **16**, 968 (1948); b) J. O. Hirschfelder, C. F. Curtiss, and R. B. Bird, "Molecular Theory of Gases and Liquids," Wiley (1954), p. 1126.

19) L. S. Tee, S. Gotoh, and W. E. Stwart, *Ind. Eng. Chem., Fundam.* **5**, 356 (1966).

20) Ref. 18b, p. 1112.

21) J. Roberts, *Brit. Chem. Eng.*, **8**, 753 (1963).

22) E. Wilhelm and R. Battino, *J. Chem. Phys.*, **55**, 4012 (1971).

23) B. S. Rabinovitch and D. W. Setser, *Adv. Photochem.*, **3**, 1 (1964).

24) P. Warneck, *Z. Naturforsch., Teil A*, **26**, 2047 (1971).

25) A. L. Castelhano, P. R. Marriott, and D. Griller, *J. Am. Chem. Soc.*, **103**, 4262 (1981).

26) F. P. Lossing and G. P. Semeluk, *Can. J. Chem.*, **48**, 955 (1970).

27) J. A. Kerr, *Chem. Rev.*, **66**, 465 (1966).

28) M. Rossi and D. M. Golden, *Int. J. Chem. Kinet.*, **11**, 969 (1979).

29) L. G. Piper, R. H. Krech, and R. L. Taylor, *J. Chem. Phys.*, **73**, 791 (1980).

30) K. Yang and T. Ree, *J. Chem. Phys.*, **35**, 588 (1961).

31) J. C. Slater and J. G. Kirkwood, *Phys. Rev.*, **37**, 682 (1931); J. G. Kirkwood, *Physik. Z.*, **33**, 57 (1932).

32) Estimated by assuming the atomic polarizabilities of 0.401×10^{-24} cm^3 for H and 0.975×10^{-24} cm^3 for N.

33) P. E. Cade and W. M. Huo, *J. Chem. Phys.*, **45**, 1063 (1966).

34) D. Husain and L. J. Kirsch, *Trans. Faraday Soc.*, **67**,

2886 (1971).

35) D. Husain and L. J. Kirsch, *Trans. Faraday Soc.*, **67**, 3166 (1971).

36) W. B. DeMore, *J. Phys. Chem.*, **73**, 391 (1969); R. J. Cvetanović, *Can. J. Chem.*, **52**, 1452 (1974); G. E. Streit, C. J. Howard, A. L. Schmeltekopf, J. A. Davidson, and H. I. Schiff, *J. Chem. Phys.*, **65**, 4761 (1976); J. A. Davidson, H. I. Schiff, T. J. Brown, G. E. Streit, and C. J. Howard, *ibid.*, **69**, 1213 (1978).

37) I. S. Fletcher and D. Husain, *Can. J. Chem.*, **54**, 1765 (1976).

38) J. A. Davidson, H. I. Schiff, G. E. Streit, J. R. McAfee, A. L. Schmeltekopf, and C. J. Howard, *J. Chem. Phys.*, **67**, 5021 (1977).

39) H. E. Gunning and O. P. Strausz, *Adv. Photochem.*, **4**, 143 (1966); P. Fowles, M. deSorgo, A. J. Yarwood, O. P. Strausz, and H. E. Gunning, *J. Am. Chem. Soc.*, **89**, 1352 (1967).

40) D. L. Little, A. Dalgleish, and R. J. Donovan, *Discuss. Faraday Soc.*, **53**, 211 (1972).

41) M. N. R. Ashfold, M. A. Fullstone, G. Hancock, and G. W. Ketley, *Chem. Phys.*, **55**, 245 (1981).

42) A. O. Langford, H. Petek, and C. B. Moore, *J. Chem. Phys.*, **78**, 6650 (1983).